1995RMxAA..31..147P

Revista Mexicana de Astronomía y Astrofísica, **31**, 147-158 (1995)

TEMPERATURE FLUCTUATIONS AND THE CHEMICAL COMPOSITION OF PLANETARY NEBULAE OF TYPE I

M. Peimbert, V. Luridiana, and S. Torres-Peimbert

Instituto de Astronomía
Universidad Nacional Autónoma de México

Received 1995 July 13; accepted 1995 September 19

RESUMEN

Presentamos dos nuevos métodos para determinar la temperatura electrónica basados en las intensidades de las líneas de He I. Las temperaturas que se obtienen a partir de estos métodos son menores que aquellas que se obtienen a partir de las líneas $\lambda\lambda$4363 y 5007 de O^{++}, esta diferencia implica la presencia de fluctuaciones espaciales de temperatura. Determinamos las abundancias en las nebulosas planetarias de tipo I de algunos de los elementos más importantes tomando en cuenta las fluctuaciones de temperatura. Encontramos que las abundancias de He^+/H^+ derivadas a partir de distintas líneas de He I son similares entre sí sin la necesidad de suponer que existe un mecanismo desconocido que reduce la población del nivel 2^3S de He I. Encontramos que los valores de He/H, C/H y N/H son mayores que en el medio interestelar; por otro lado encontramos que el valor de O/H es similar al de las estrellas recién formadas y que el valor de Ar/O es similar al de las regiones H II de la vecindad solar (Orion y M17), estos resultados indican que no hay evidencia en favor de una disminución del O en las envolventes producida por reacciones nucleares en la estrella central.

ABSTRACT

We present two new methods to determine the electron temperature based on the He I line intensities. The temperatures derived from these methods are considerably smaller than those derived from the [O III] $\lambda\lambda$4363, 5007 line intensities and imply the presence of large spatial temperature fluctuations in PNe. Considering the presence of spatial temperature fluctuations we determine the abundance of some of the most important elements in Type I PNe. The He^+/H^+ values derived from different He I lines come into agreement without the need of invoking an unknown process depopulating the 2^3S He I level. We find He, C and N overabundances; alternatively we find that the O/H value is similar to that of stars recently formed, moreover we also find that the Ar/O value is similar to that of H II regions of the solar vicinity (Orion and M17), these results imply that there is no evidence in favor of a decrease of the O abundance in the nebular shells due to nuclear reactions in the central stars.

Key words: **ISM – ABUNDANCES — PLANETARY NEBULAE**

1. INTRODUCTION

The presence of spatial temperature fluctuations in PNe is well established (Peimbert 1995, and references therein). Type I PNe show systematically larger temperature fluctuations than other types of PNe (Peimbert, Torres-Peimbert, & Luridiana 1995, hereinafter Paper II), therefore Type I PNe are bound to show the largest errors in their abundance determinations if temperature fluctuations are not taken into account. It is the purpose of this paper to explore the effect of temperature fluctuations on the determination of the chemical composition of the sample of PNe of Type I presented by Peimbert & Torres-Peimbert (1987a, hereinafter Paper I).

It has been found in previous work that different

© Universidad Nacional Autónoma de México • Provided by the NASA Astrophysics Data System

1995RMxAA..31..147P

He I lines yield different He^+/H^+ abundances. The differences imply that the collisional excitations from the He I 2^3S level have been overestimated. There are several possible solutions to this problem: a) there is an unknown mechanism depopulating the 2^3S level, b) the density has been overestimated and c) the temperature has been overestimated. Type I PNe are important objects to study this problem since they show extreme temperature fluctuations.

In § 2 we will study the presence of temperature fluctuations based on the He I line intensities. In § 3 we will determine the He/H value for the sample of Type I PNe in Paper I. In § 4 we will determine ionic and total abundances of some heavy elements for the sample. The conclusions will be presented in § 5.

2. HELIUM LINES AND ELECTRON TEMPERATURE

The $N(He^+)/N(H^+)$ ratios can be derived from

$$\frac{N(He^+)}{N(H^+)} = \frac{\alpha(H^0, H\beta)}{\alpha(He^0, \lambda_{nm})} \frac{\lambda_{nm}}{4861} \frac{I(\lambda_{nm})_R}{I(H\beta)} \quad , \qquad (1)$$

where the effective recombination coefficients, α, for hydrogen and helium have been computed by Hummer & Storey (1987) and Smits (1995), and $I(\lambda_{nm})_R$ is the pure recombination intensity that has to be obtained from the observed intensity corrected for reddening, $I(\lambda_{nm})$. Collisions and radiative transfer effects from the 2^3S of He I level affect $I(\lambda_{nm})$ and have to be estimated.

The collisions to recombination ratio of a helium line is given by

$$\frac{I(\lambda_{nm})_C}{I(\lambda_{nm})_R} = \frac{N(2^3S)\kappa(\lambda_{nm})}{N(He^+)\alpha(\lambda_{nm})} \quad , \qquad (2)$$

where κ is the effective collisional coefficient that depends strongly on T_e and

$$\frac{N(2^3S)}{N(H^+)} = \frac{5.62 \times 10^{-6} t_4^{-1.19}}{1 + 3130 t_4^{-0.5} N_e^{-1}} \quad , \qquad (3)$$

where ionizations from the 2^3S level have been neglected (Kingdon & Ferland 1995).

The latest estimates of the $I(\lambda_{nm})_C/I(\lambda_{nm})_R$ values, C/R, for the different helium lines are those by Kingdon & Ferland (1995) which are based on the 29-state ab initio computation for collisions to He^0 states with $n \leq 5$ by Sawey & Berrington (1993) and the helium recombination coefficients by Smits (1995).

We have derived an equation for $\lambda(10830)$ given by

$$\frac{I_C(10830)}{I_R(10830)} =$$

$$\left(29.00 t_4^{-0.04}\, e^{-1.330/t_4} + 2.56 t_4^{-0.81}\, e^{-3.364/t_4}\right.$$

$$\left. +2.22 t_4^{-0.14}\, e^{-3.776/t_4}\right)/(1 + 3130 t_4^{-0.5} N_e^{-1}) , \qquad (4)$$

where we have considered the 2^3P, 3^3S and 3^3D terms, the other terms contribute less than 1% to $I_C(10830)$. To derive equation (4) we considered the ab initio computation by Sawey & Berrington (1993) and the $\alpha(10830)$ value by Robbins (1968a). We did not use the results by Brocklehurst (1972) because the error in the 2^3P - n^3S series (Smits 1991) affects the $\alpha(10830)$ value.

If there is an additional process depopulating the 2^3S level, the $N(2^3S)$ population would be a fraction γ of that given by equation (3) and the I_C/I_R ratios would be simply γ times those given by equation (2).

The $I(\lambda_{nm})$ dependence on temperature, for $N_e \geq 3000$ cm^{-3}, due to collisional effects is strong for $\lambda\lambda$10830 and 7065, moderate for $\lambda\lambda$3889 and 5876 and weak for $\lambda\lambda$4471 and 6678.

Robbins (1968b) and Robbins & Bernat (1973) have computed the effect that atomic absorption has on the He I line intensity ratios. Robbins used as a parameter for the triplet series $\tau(3889)$, the He I λ3889 optical depth. From the computations by Robbins, and Cox & Daltabuit (1971) and the ratio of two He I lines it is possible to determine $\tau(3889)$ and consequently the effect of the radiation transfer on the triplet lines. A similar procedure can be followed for the singlet lines. It is found that radiative transfer effects for typical PNe are large for $\lambda\lambda$3889 and 7065, are small for $\lambda\lambda$5876 and 10830 and almost negligible for $\lambda\lambda$4471 and 6678.

2.1. The Hu 1–2 *Electron Temperature Derived from the* He I *Lines*

Hu 1–2 is the best object of the sample in Paper I to determine the electron temperature from the He I lines, because the collisional effects are very large due to its high density and high temperature.

In Table 1 we have determined the $N(He^+)/N(H^+)$ values for Hu 1–2 under different assumptions; the values correspond to the average of positions a, b and c. In column 2 we present the case for pure recombination (no collisions from the 2^3S level), $\tau(3889) = 0.00$, $\langle T_e \rangle = 18\,420$ K and $\langle N_e \rangle = 4400$ cm^{-3}. There is no agreement among $y^+(4471)$, $y^+(5876)$ and $y^+(6678)$, where $y^+(\lambda_{nm}) = N(He^+, \lambda_{nm})/N(H^+)$. We do not take into account $y^+(3889)$ and $y^+(7065)$ because they depend on $\tau(3889)$ and have higher observational errors. In column 3 we present the case of full collisional corrections for $\tau(3889) = 0.00$, $\langle T_e \rangle = 18\,420$ K and $\langle N_e \rangle = 4400$ cm^{-3}; in this case the collisional ef-

© Universidad Nacional Autónoma de México • Provided by the NASA Astrophysics Data System

1995RMxAA..31..147P

TABLE 1

He^+/H^+ ABUNDANCE RATIO FOR Hu 1–2

λ	$\gamma = 0^a$	$\gamma = 1^b$	$\gamma = 1^c$	$\gamma = 1^d$
3889	0.0739	0.0462	0.0622	0.0679
4471	0.0696	0.0476	0.0592	0.0591
5876	0.0808	0.0475	0.0610	0.0608
6678	0.0693	0.0569	0.0592	0.0592
7065	0.1846	0.0580	0.0925	0.0753

[a] Pure recombination, $\langle T_e \rangle$ = 18 420 K, t^2 = 0.00, τ(3889) = 0 and $\langle N_e \rangle$ = 4400 cm^{-3}.
[b] Full collisional corrections, $\langle T_e \rangle$ = 18 420 K, t^2 = 0.00, τ(3889) = 0 and $\langle N_e \rangle$ = 4400 cm^{-3}.
[c] Full collisional corrections, $\langle T_e \rangle$ = 12 490 K, $t^2 \neq$ 0.00, τ(3889) = 0 and $\langle N_e \rangle$ = 4400 cm^{-3}.
[d] Full collisional corrections, $\langle T_e \rangle$ = 12 490 K, $t^2 \neq$ 0.00, τ = 3.5 and $\langle N_e \rangle$ = 4400 cm^{-3}

fects have been overestimated because $y^+(6678)$ is higher than $y^+(5876)$ and $y^+(4471)$. There are at least three solutions to this contradiction: a) there is an unknown process depopulating the 2^3S level (i.e., $\gamma < 1$), this possibility has been studied by Clegg & Harrington (1989) who find that photoionization can reduce the $N(2^3S)$ population by as much as 25% in compact optically thick PNe, alternatively they find that for the vast majority of the typical PNe the effect is very small and can be neglected, b) the density has been overestimated, this possibility could be important for objects with $N_e \leq 3000$ cm^{-3}, but probably for Hu 1–2 is not important (see equation [3]), c) the temperature has been overestimated.

In column 4 of Table 1 we find that for T_e = 12 490 K the $y^+(6678)$, $y^+(5876)$ and $y^+(4471)$ values are in excellent agreement. In column 5 of Table 1 we find that for $\tau(3889) \neq 0$ the $y^+(6678)$, $y^+(5876)$ and $y^+(4471)$ values are almost unaffected by changes on $\tau(3889)$, while $y^+(3889)$ and $y^+(7065)$ depend strongly on $\tau(3889)$; the differences between $y^+(7065)$ and $y^+(3889)$ relative to the other three values probably are due to observational errors (see § 3).

In Figure 1 we present the $y^+(4471)$, $y^+(5876)$ and $y^+(6678)$ values as a function T_e for $\tau(3889) = 0.00$ and with full collisional corrections. As can be seen from Table 1 these y^+ values are almost independent of $\tau(3889)$. The temperature at which the three lines reach the same y^+ value is in the 12 500 to 13 500 K range, a value considerably smaller than that given by $\langle T_e \rangle$ (4363/5007) that amounts to 18 420 ± 600 K; this result implies a very large mean square temperature fluctuation, t^2, value. The T_e(He) value derived from Figure 1 (see also Table 1), is in excellent agreement with $T(C^{++})$ = 12 490 K derived from the $\lambda\lambda$4267/(1906 + 1909) intensity ratio (see Paper II) and probably implies that shock waves are present in Hu 1–2 .

Peña et al. (1995), from a similar study of N66, a Type I PN in the Large Magellanic Cloud, also find that lower T_e and N_e values, than those given by the [O III], [O II] and [Ar IV] lines, are needed to derive the same y^+ values from the $\lambda\lambda$ 4471, 5876 and 6678 lines.

2.2. τ(3889) vs. T_e

As mentioned before I(3889), I(7065) and I(10830) depend strongly on the collisional effects from the 2^3S level and on τ(3889), while I(4471) does not; consequently the $I(3889)/I(4471)$,

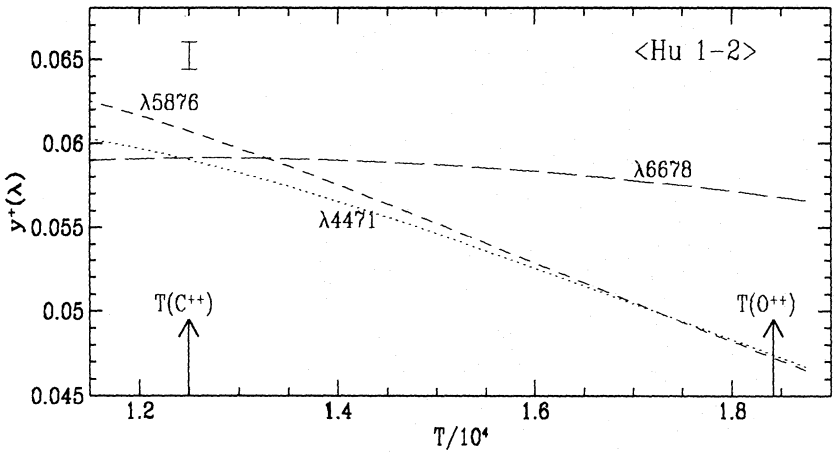

Fig. 1. $N(He^+)/N(H^+) = y^+(\lambda)$ vs. T diagram for the Type I PN Hu 1–2, where we have used the average helium to hydrogen line intensity ratios of three different regions of the nebula. The y^+ values are presented for $\lambda\lambda$4471, 5876 and 6678 together with an error bar for the y^+ values.

© Universidad Nacional Autónoma de México • Provided by the NASA Astrophysics Data System

1995RMxAA..31..147P

$I(7065)/I(4471)$ and $I(10830)/I(4471)$ ratios also depend on $\tau(3889)$ and T_e. For any given value of $\tau(3889)$ there is only one value of T_e that will match the observed ratio with the computed one. The relationship between $\tau(3889)$ and T_e for any line ratio is derived by comparing the observed ratio with the computed one based on the corresponding C/R relation and the computations by Robbins (1968b). The three line ratios depend on different functions of $\tau(3889)$ and T_e, therefore the combination of two line ratios will provide us with a unique pair of $\tau(3889)$ and T_e values.

In general each line ratio will be given by

$$\frac{I(\lambda_{nm})}{I(\lambda_{n'm'})} = \frac{(I_R + I_C)\, j(\tau)\, j'(0)}{(I'_R + I'_C)\, j(0)\, j'(\tau)} = \frac{I_R(1 + C/R)}{I'_R(1 + C'/R')} \frac{j(\tau)}{j(0)} \frac{j'(0)}{j'(\tau)} \quad , \quad (5)$$

where the C/R values were obtained from Kingdon & Ferland (1995) or equation (4), I_R/I'_R from Smits (1995) or Robbins (1968a) and the emissivity ratios, $j(\tau)/j(0)$, from Robbins (1968b), where $j(0)$ is the value for $\tau(3889) = 0$.

In Figure 2 we present $\tau(3889)$ vs. T_e diagrams for six PNe with high quality observations of $\lambda\lambda$ 3889, 4471, 7065 and 10830 (Peimbert & Torres-Peimbert 1987b, and references therein). From these diagrams we obtain $T_e(\lambda_{nm}, \lambda_{n'm'})$ values based on pairs of $I(\lambda_{nm})/I(4471)$ intersections, we adopted errors of 0.04 dex in the line intensity ratios; the results are presented in Table 2. In Figure 2 we adopted the emissivity ratios computed by Robbins (1968b) for $v(\mathrm{exp})/v(\mathrm{ther}) = 3$, where $v(\mathrm{exp})$ is the velocity of expansion of the nebula and v (ther) is the thermal velocity; for $v(\mathrm{exp})/v(\mathrm{ther}) = 0$ the τ values decrease by about a factor of 2 but the T_e values remain about the same. Also in Table 2 we include the $T(\mathrm{O}^{++})$ and N_e values presented in Paper I, the $T(\mathrm{C}^{++})$ values

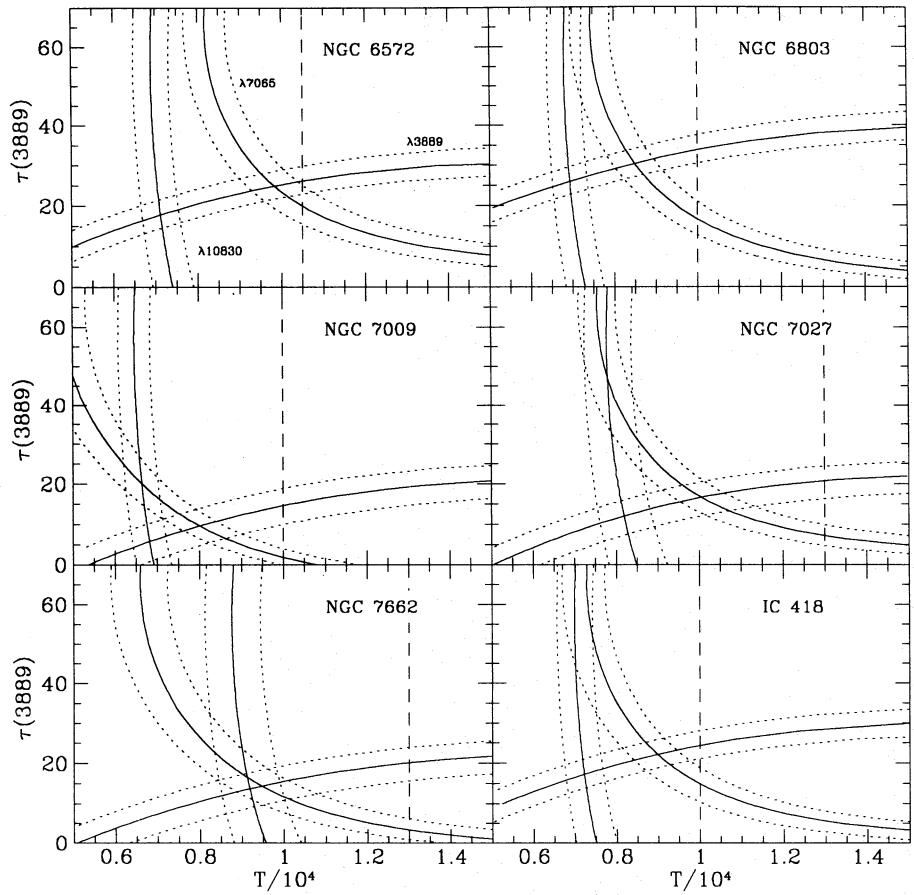

Fig. 2. $\tau(3889)$ vs. T diagram for six PNe. The solid lines stand for the $I(\lambda)/I(4471)$ ratio; the dotted lines to the right of the solid lines correspond to line intensity ratios 10% higher than observed; while the dotted lines to the left correspond to line intensity ratios 10% lower than observed. The vertical dashed lines correspond to $T(\mathrm{O}^{++})$.

© Universidad Nacional Autónoma de México • Provided by the NASA Astrophysics Data System

1995RMxAA..31..147P

TABLE 2

TEMPERATURE DERIVED FROM OXYGEN, CARBON AND HELIUM LINES

PN	N_e (cm^{-3})	$T(O^{++})$ (K)	$T(C^{++})$ (K)	T(3889,7065) (K)	T(3889,10830) (K)	T(7065,10830) (K)
NGC 6572	21000	10500	9820	9800 ± 600	7100 ± 500	...
NGC 6803	9000	10000	...	8500 ± 500	6900 ± 400	...
NGC 7009	6000	10000	8320	8000 ± 400	6800 ± 400	6600 ± 500
NGC 7027	80000	13000	12430	10000 ± 600	8200 ± 600	8000 ± 500
NGC 7662	4000	13000	12200	9500 ± 600	9200 ± 700	9100 ± 800
IC 418	15000	10000	8450	9000 ± 600	7200 ± 500	...

from Paper II and the $T(C^{++})$ value for IC 418 derived from Paper II and the line intensities obtained by Torres-Peimbert, Peimbert, & Daltabuit (1980).

From the $I(3889)/I(7065)$ intersections we obtain T_e values systematically higher than from the $I(3889)/I(10830)$ and $I(7065)/I(10830)$ intersections; the differences could be due to dust destruction inside the PNe and to telluric absorption of λ10830 photons (Clegg & Harrington 1989; Kingdon & Ferland 1991, 1993). Although telluric absorption in the 7065 line would have the effect of moving the 7065 curve to the right in Figure 2, this effect is insufficient to account for the observed discrepancy between $T(He^+)$ and $T(O^{++})$.

In all cases the temperature derived from the $I(3889)/I(7065)$ intersections, T(3889, 7065), is smaller than $T(O^{++})$ and in three cases is similar to $T(C^{++})$ (see Table 2). In particular the T(3889,7065) value for NGC 7009 is in excellent agreement with the T(Bac) values derived by Peimbert (1971) and Liu & Danziger (1993) —that amount to 7600 ± 900 K and 8760 ± 1300 K respectively— and with the $T(C^{++})$ value (see Table 2).

3. He^+/H^+ IN TYPE I PNe

In Table 3 we present the adopted N_e and T_e values for the PNe of Type I studied in Paper I.

TABLE 3

TEMPERATURES AND DENSITIES

Object	$T(O^{++})$ (K)	$T(C^{++})$ (K)	$T(N^+)$ (K)	N_e (cm^{-3})
NGC 650–1	11990	(9590)[a]	9950	1000
NGC 2346	11270	(9200)	9010	700
NGC 2371	13175	9840	9790	500
NGC 2440a	14810	12650	10890	4500
NGC 2440b	13995	12650	9640	1900
NGC 2818	15100	11660	12430	500
NGC 7293	10190	(8420)	8240	100
Hu 1–2a	18705	12490	13260	5000
Hu 1–2b	18260	12490	13280	4700
Hu 1–2c	18310	12490	13310	3400
M1–8	12710	(10050)	12610	320
M1–13	10690	(8810)	10540	2100
M1–17	10970	(9070)	11110	5300
M2–55	10110	(8380)	10900	460
M3–3	11860	(9530)	9000	300
Me2–2	10950	(9230)	10560	40000

[a] The values in parenthesis are based on equation (6).

© Universidad Nacional Autónoma de México • Provided by the NASA Astrophysics Data System

1995RMxAA..31..147P

TABLE 4

He^+/H^+ ABUNDANCE RATIOS WITHOUT CORRECTIONS

Object	$y^+(3889)$	$y^+(4471)$	$y^+(5876)$	$y^+(6678)$	$y^+(7065)$	$\langle y^+\rangle^a$
NGC 650–1	0.0980	0.0909	0.1041	0.0886	0.114	0.0945
NGC 2346	0.0862	0.1084	0.1097	0.0990	...	0.1057
NGC 2371–2	0.0488	0.0376	0.0396	0.0399	0.0409	0.0390
NGC 2440a	0.0568	0.0563	0.0649	0.0628	0.1280	0.0613
NGC 2440b	0.0996	0.0893	0.1092	0.1057	...	0.1014
NGC 2818	0.0910	0.0950	0.1162	...	...	0.1056
NGC 7293	0.1094	0.1287	0.1426	...	...	0.1357
Hu 1–2a	0.0834	0.0711	0.0869	0.0719	0.1923	0.0766
Hu 1–2b	0.0799	0.0727	0.0848	0.0761	0.2033	0.0779
Hu 1–2c	0.0585	0.0651	0.0708	0.0599	0.1581	0.0653
M1–8	...	0.0945	0.1107	...	...	0.1026
M1–13	0.0944	0.1142	0.1107	0.0942	0.1439	0.1064
M1–17	0.0622	0.1095	0.1178	0.1085	0.2782	0.1119
M2–55	0.0968	0.1192	0.1083	...	...	0.1138
M3–3	0.0983	0.1062	0.1004	0.0822	...	0.0963
Me2–2	0.0642	0.1618	0.1907	0.1754	0.6990	0.1760

[a] Average of $\lambda\lambda$4471, 5876 and 6678.

We recomputed the $T(O^{++})$ and $T(N^+)$ values from the line intensities presented in Paper I and we adopted the $T(N^+)$ value for M3–3 derived by Kaler, Shaw, & Kwitter (1990). Based on the PNe of Type I with $T(C^{++})$ determinations presented in Paper II (NGC 2371–2, NGC 2440, NGC 2818, NGC 6153,NGC 6302, NGC 6543, NGC 6565 and Hu 1–2) we derived the following relation

$$T(C^{++}) = 0.654T(O^{++}) + 1681 \quad ; \qquad (6)$$

from equation (6) we determined the $T(C^{++})$ values in parenthesis in Table 3; all the other values in this table come from Papers I and II.

In Table 4 we present the derived helium abundance values without corrections from collisional and self absorption effects. As discussed in § 2 and in Paper II we consider that $T(C^{++})$ is more representative for determining the He^+/H^+ values than $T(O^{++})$. In all cases the Pickering contribution of the He II lines to the Balmer H I lines was taken into account. From this table it can be seen that in general $y^+(5876)$ and $y^+(7065)$ are higher than $y^+(4471)$ and $y^+(6678)$. The average value, $\langle y^+\rangle$, is based on the three lines less affected by collisions and self absorption effects.

In Table 5 we present the helium abundance values with full collisional corrections, $\gamma = 1$, and considering self absorption effects. $\tau(3889)$ was computed based mainly on $\lambda\lambda$3889 and 7065 and adopting $v(\exp)/v(\text{ther}) = 3.0$ (Robbins 1968b). The differences between $y^+(\lambda_{nm})$ and $\langle y^+\rangle$ are of the order of the observational errors and there is no need to invoke an unknown mechanism to reduce the population of the 2^3S level.

The $\langle y^+\rangle$ values for the objects in Table 5 are lower than those in Table 4, the $\langle y^+\rangle$ ratio varies from 0.80 to 0.96. The $\langle y^+\rangle$ values are almost independent of $\tau(3889)$, consequently most of the difference is due to collisional effects (see Table 1).

The total helium abundance is given by

$$\frac{N(He)}{N(H)} = \frac{N(He^0 + He^+ + He^{++})}{N(H^0 + H^+)} \quad , \qquad (7)$$

for objects of low degree of ionization there is an outer He^0 zone within the H^+ zone, alternatively for objects of high degree of ionization there is an outer H^0 zone within the He^+ zone and no He^0 zone. If one is dealing with a density bounded nebula the He^0 and H^0 zones can disappear. We did not consider the He^0 and H^0 terms in equation (7) for the objects in this paper. Nevertheless it is likely that those objects with large $N(S^+)/N(H^+)$ values might have significant amounts of He^0 present.

In Table 6 we present the total helium to hydrogen abundance ratios. The He^{++}/H^+ values were derived from the $I(4686)/I(4861)$ line intensity ratios and the computations by Hummer & Storey (1987) adopting $T(C^{++})$; probably the regions where the

© Universidad Nacional Autónoma de México • Provided by the NASA Astrophysics Data System

1995RMxAA..31..147P

TABLE 5

CORRECTED He^+/H^+ ABUNDANCE RATIOS AND $\tau(3889)$ VALUES

Object	$y^+(3889)$	$y^+(4471)$	$y^+(5876)$	$y^+(6678)$	$y^+(7065)$	$\langle y^+\rangle^a$	$\tau(3889)$
NGC 650–1	0.0970	0.0865	0.0947	0.0819	0.0921	0.0877	0.0
NGC 2346	0.1029	0.1036	0.1007	0.0922	...	0.0988	7.0
NGC 2371–2	0.0505	0.0356	0.0357	0.0365	0.0382	0.0359	0.0
NGC 2440a	0.0512	0.0483	0.0498	0.0552	0.0441	0.0511	5.0
NGC 2440b	0.0893	0.0806	0.0912	0.0968	...	0.0895	2.0
NGC 2818	0.0950	0.0896	0.1042	...	...	0.0969	2.0
NGC 7293	0.1309	0.1249	0.1344	...	...	0.1297	6.0
Hu 1–2a	0.0766	0.0599	0.0646	0.0611	0.0752	0.0619	4.0
Hu 1–2b	0.0717	0.0615	0.0635	0.0649	0.0839	0.0633	3.0
Hu 1–2c	0.0555	0.0559	0.0542	0.0516	0.0669	0.0539	4.0
M1–8	...	0.0906	0.1022	...	...	0.0964	0.0
M1–13	0.1035	0.1086	0.1004	0.0874	0.0837	0.0988	5.0
M1–17	0.1024	0.1019	0.1021	0.0991	0.0799	0.1010	22.2
M2–55	0.1047	0.1153	0.1016	...	...	0.1085	2.5
M3–3	0.1045	0.1021	0.0931	0.0767	...	0.0906	1.5
Me2–2	0.1420	0.1469	0.1575	0.1577	0.1332	0.1540	35.0

[a] Average of $\lambda\lambda$4471, 5876 and 6678.

TABLE 6

HELIUM ABUNDANCES[a]

Object	He^+	He^{++}	He
NGC 650–1[b]	0.088	0.035	>0.123
NGC 2346	0.099	0.033	0.132
NGC 2371–2	0.036	0.081	0.117
NGC 2440a	0.051	0.072	0.123
NGC 2440b	0.090	0.046	0.136
NGC 2818	0.097	0.066	0.163
NGC 7293	0.130	<0.002	0.130
Hu 1–2a	0.062	0.089	0.151
Hu 1–2b	0.063	0.089	0.152
Hu 1–2c	0.054	0.098	0.152
M1–8	0.096	0.051	0.147
M1–13	0.099	0.015	0.114
M1–17	0.101	0.012	0.113
M2–55	0.109	0.028	0.137
M3–3	0.091	0.030	0.121
Me2–2	0.154	0.000	0.154

[a] Given in $N(He^i)/N(H^+)$.

[b] Probably has a significant amount of He^0 inside the H^+ zone.

He II lines originate are hotter than the regions where the He I lines originate, but we do not have any direct measurement of T_e for the He^{++} region. Higher T_e values would yield slightly higher He^{++}/H^+ values.

4. THE HEAVY ELEMENTS

To compute the heavy element abundances relative to those of H we used the compilation of atomic parameters by Mendoza (1983) and the H I and He II effective recombination coefficients for case B by Hummer & Storey (1987).

The ionic abundances were derived adopting a three temperature scheme: for N^+, O^+ and S^+ we used $T(N^+)$; for C^{++}, O^{++}, Ne^{++}, S^{++}, Ar^{++}, Ar^{3+} and Cl^{++} we used $T(C^{++})$; and for He^{++}, Ne^{3+} and Ar^{4+} we used $T(O^{++})$. We made use of $T(O^{++})$ because for higher ionized species we expect larger T_e values (e.g. Shields et al. 1981), furthermore the Ne^{3+} abundances were derived from the $\lambda\lambda$4724+4726 auroral lines, which have a similar excitation energy to that of the λ4363 O^{++} line, and consequently have a similar dependence on T_e in the presence of spatial temperature fluctuations. For all ions we used the densities presented in Table 3. The ionic abundances are presented in Table 7.

In Figure 3 we present the Ne^{++}/O^{++} vs. Ne diagram. To derive the Ne/O value the following equation is often used

© Universidad Nacional Autónoma de México • Provided by the NASA Astrophysics Data System

1995RMxAA..31..147P

TABLE 7

IONIC ABUNDANCES[a]

Object	C^{++}	N^{+}	O^{+}	O^{++}	Ne^{++}	Ne^{3+}	S^{+}	S^{++}	Ar^{++}	Ar^{3+}	Ar^{4+}	Cl^{++}
NGC 650–1	−3.12	−3.96	−3.58	−3.30	−3.67	−4.35	−5.51	−4.97	−5.49	−6.69	...	−6.66
NGC 2346	−3.09	−4.16	−3.69	−3.26	−3.65	−3.49	−6.74	−5.29	...	−6.28	...	...
NGC 2371–2	−3.21	−4.82	−4.43	−3.40	−3.96	−3.73	−6.26	−4.95	−5.66	−5.57	−6.31	−6.81
NGC 2440a	−3.33	−4.08	−4.28	−3.66	−4.33	−4.14	−6.29	−5.64	−5.87	−5.96	−6.32	−7.21
NGC 2440b	−3.36	−3.66	−3.86	−3.63	−4.21	−4.07	−5.90	−5.58	...	−6.15	...	−7.14
NGC 2818	−3.39	−4.27	−4.19	−3.57	−4.01	−4.42	−5.95	−4.90	...	−6.20	...	...
NGC 7293	...	−3.65	−3.24	−3.49	−3.69	...	−6.16	...	−5.37	...	...	...
Hu 1–2a	−3.73	−4.79	−4.86	−3.88	−4.41	−4.63	−6.52	−5.47	−6.20	−6.07	−6.70	...
Hu 1–2b	...	−4.83	−4.89	−3.86	−4.42	−4.58	−6.55	−5.50	−6.17	−6.07	−6.73	...
Hu 1–2c	...	−4.89	−5.06	−3.91	−4.54	...	−6.63	−5.45	−6.16	−6.01	−6.64	...
M1–8	−2.99	−4.52	−4.29	−3.38	−3.85	...	−6.61	−5.27	...	−6.07	...	...
M1–13	...	−4.21	−3.87	−3.22	−3.70	...	−6.17	...	−5.59	−6.26	...	−6.78
M1–17	−3.12	−4.53	−4.25	−3.17	−3.79	...	−5.93	−5.01	−5.66	−6.11	−7.18	−6.71
M2–55	...	−4.34	−3.99	−3.25	−3.61	...	−6.11	...	−5.43	...	...	...
M3–3	−3.11	−3.63	−3.74	−3.44	−3.87	...	−6.53	...	...	−6.68	...	...
Me2–2	−3.15	−4.62	−4.24	−3.56	−4.08	−4.70	−6.80	−5.72	−5.98	−6.76	...	...

[a]Given in $\log N(X^{+m})/N(H^{+})$.

$$\frac{N(Ne)}{N(O)} = \frac{N(Ne^{++})}{N(O^{++})} \quad , \tag{8}$$

(e.g., Peimbert, Torres-Peimbert, & Ruiz 1992; Clegg 1993 and references therein). In Figure 3 it can be seen that Ne^{++}/O^{++} increases with decreasing density, indicating that for objects with $N_e \leq 1000\ cm^{-3}$ equation (8) is a poor approximation to the Ne/O value; this result probably is due to the presence of the charge exchange reaction

$$O^{+2} + H^{0} \rightarrow O^{+} + H^{+} \quad ,$$

that permits the coexistence of Ne^{++} with O^{+} (e.g., Hawley & Miller 1977, 1978; Hawley 1978; Pequignot, Aldrovandi, & Stasińska 1978; Butler, Bender, & Dalgarno 1979; Pequignot 1980). Ionization structure models predict that the lower the density the higher the H^{0}/H^{+} ratio, in agreement with the charge exchange suggestion and Figure 3.

To derive the total abundances presented in Table 8 we made use of equation (8) and the following equations

$$\frac{N(O)}{N(H)} = \left[\frac{N(He^{+} + He^{++})}{N(He^{+})}\right]^{2/3} \frac{N(O^{+} + O^{++})}{N(H^{+})} \quad , \tag{9}$$

$$\frac{N(C)}{N(O)} = \frac{N(C^{++})}{N(O^{++})} \quad , \tag{10}$$

$$\frac{N(N)}{N(O)} = \frac{N(N^{+})}{N(O^{+})} \quad , \tag{11}$$

$$\frac{N(Ne)}{N(H)} = \frac{N(Ne^{++} + Ne^{3+})}{N(H^{+})} \quad , \tag{12}$$

$$\frac{N(Ar)}{N(H)} = i_{cf}(Ar)\frac{N(Ar^{++} + Ar^{3+} + Ar^{4+})}{N(H^{+})} \quad , \tag{13}$$

where

$$i_{cf}(Ar) = \left[1 - \frac{N(N^{+})}{N(N)}\right]^{-1} \quad . \tag{14}$$

and

$$\frac{N(Ar)}{N(H)} = 1.87\frac{N(Ar^{++})}{N(H^{+})} \quad . \tag{15}$$

Equation (9) comes from Kingsburgh & Barlow (1994). Equation (10) is a fair approximation to the C/O ratio: from ionization structure models it

© Universidad Nacional Autónoma de México • Provided by the NASA Astrophysics Data System

1995RMxAA..31..147P

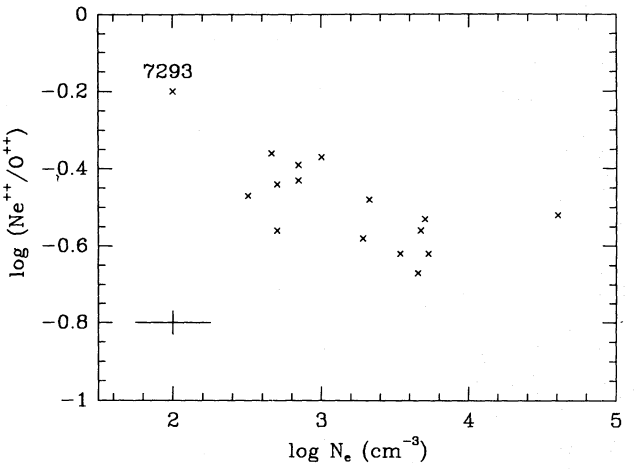

Fig. 3. Ne^{++}/O^{++} vs. electron density N_e. A typical error is presented.

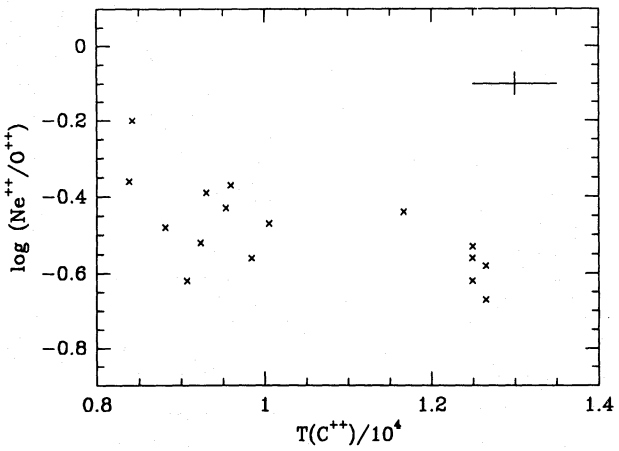

Fig. 4. Ne^{++}/O^{++} vs. $T(C^{++})$.

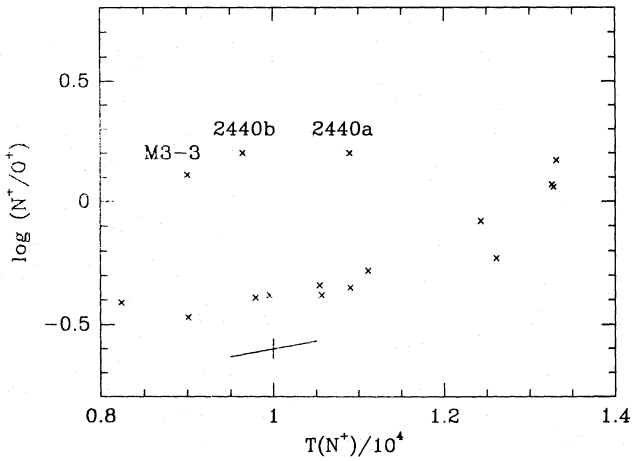

Fig. 5. N^+/O^+ vs. $T(N^+)$. A typical error is presented, where the dependence of N^+/O^+ on temperature is considered. The vertical bar corresponds to an error in the $I(6583)/I(3727)$ ratio of 0.04 dex.

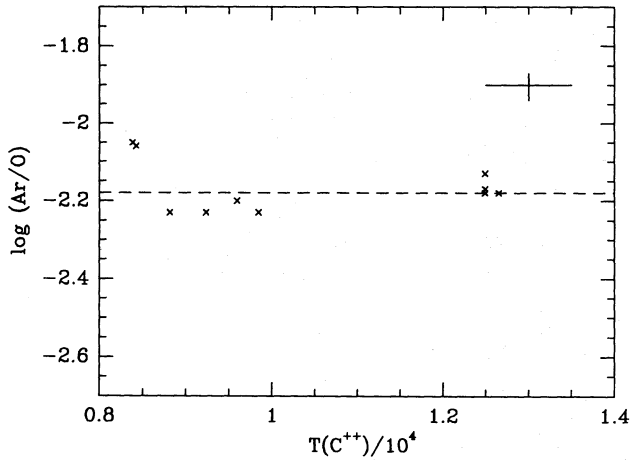

Fig. 6. Ar/O vs. $T(C^{++})$.

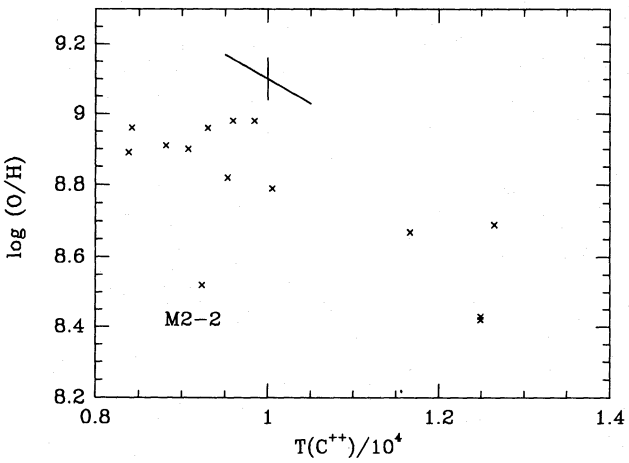

Fig. 7. O/H vs. $T(C^{++})$.

© Universidad Nacional Autónoma de México • Provided by the NASA Astrophysics Data System

1995RMxAA..31..147P

TABLE 8

TOTAL ABUNDANCES[a]

Object	C[b]	C[c]	N	O	Ne[d]	Ne[e]	Ar
NGC 650–1	>8.88	9.16	>8.60	8.98	>8.61	8.41	6.78
NGC 2346	>8.91	9.13	>8.49	8.96	>8.57	8.74:	...
NGC 2371–2	>8.79	9.17	>8.59	8.98	>8.42	8.47	6.75
NGC 2440a	>8.67	9.02	8.89	8.69	8.02	8.08	6.51
NGC 2440b	>8.64	8.96	8.89	8.69	8.11	8.17	...
NGC 2818	>8.61	8.85	>8.59	8.67	>8.23	8.13	...
NGC 7293	...	...	>8.55	8.96	>8.76	...	6.90
Hu 1–2a	>8.27	8.57	8.49	8.42	7.89	7.79	6.25
Hu 1–2b	...	...	8.49	8.43	7.87	7.81	6.25
Hu 1–2c	...	...	8.59	8.42	7.79	...	6.29
M1–8	>9.01	9.18	>8.56	8.79	>8.32	...	...
M1–13	...	...	8.57	8.91	8.43	...	6.68
M1–17	>8.88	8.95	8.62	8.90	8.28	...	6.51
M2–55	...	...	>8.54	8.90	>8.53	...	6.84
M3–3	>8.89	9.15	>8.93	8.82	>8.39	...	...
Me2–2	>8.85	8.93	8.14	8.52	8.00	8.01	6.29

[a] Given in log $N(X)/N(H) + 12$.
[b] Given by $N(C)/N(H) = N(C^{++})/N\ H^{+})$.
[c] Given by $N(C)/N(O) = N(C^{++})/N(O^{++})$.
[d] Given by $N(Ne)/N(O) = N(Ne^{++})/N(O^{++})$.
[e] Given by $N(Ne)/N(H) = N(Ne^{++} + Ne^{3+})/N(H^{+})$.

is found that $C/O \approx C^{++}/O^{++}$ (e.g., Shields et al. 1981; Harrington et al. 1982); alternatively if the $O^{++} + H^0 \rightarrow O^+ + H^+$ reaction becomes very important then $C/O < C^{++}/O^{++}$. Moreover if T_e is smaller than the adopted value C^{++}/O^{++} will decrease even further. Equation (11) has been used often for PNe and H II regions (e.g., Peimbert & Costero 1969); if a lower temperature than $T(N^+)$ is adopted then N/O decreases. Alternatively if the $O^{++} + H^0 \rightarrow O^+ + H^+$ reaction affects significantly the O^{++}/O^+ value then equation (11) provides a lower limit to the N/O ratio; the N/O value is marked as a lower limit in Table 8 for those objects with $N_e \leq 1000\ cm^{-3}$. As mentioned before equation (8) seems to be a poor approximation to the Ne/O values of these objects, equation (12) seems to be a better approximation since the fractions of Ne^+ and Ne^{4+} are very small in comparison with the Ne^{++} and Ne^{3+} fractions; the Ne^{3+} fractions are very uncertain because they depend significantly on T_e, furthermore the $\lambda\lambda 4724 + 4726$ [Ne IV] line intensities are in general poorly known. Equations (14) and (15) come from Kingsburgh & Barlow. To derive the Ar abundances in Table 8 we made use of equation (15) for NGC 650, NGC 7293, M1–13, M2–55 and Me2–2, while for the other six we used equations (13) and (14).

In Figure 4 we present the Ne^{++}/O^{++} vs. $T(C^{++})$ diagram. In this figure it can also be seen that the lower the $T(C^{++})$ value the higher the Ne^{++}/O^{++} ratio. This trend could be due to the $O^{++} + H^0 \rightarrow O^+ + H^+$ reaction, since in general the lower the density the lower the $T(C^{++})$ value and the higher the importance of the charge exchange reaction.

In Figure 5 we present the N^+/O^+ value. With the exception of NGC 2440 and M3–3 there is a tight correlation for all the other objects. This correlation seems to be a combination of many factors: a) observational selection against objects with $N/O < -0.4$ dex, b) errors in T_e run almost parallel to the correlation (see error box in the figure), c) probably hotter stars tend to be more massive and during their evolution produce higher N/O values; a larger sample of objects with accurate observations as well as ionization structure models for each object are needed to see if this correction is real.

In Figure 6 we present the Ar/O vs. $T(C^{++})$ diagram. It can be seen from this figure that there are no systematic effects due to $T(C^{++})$ affecting the Ar/O determinations. Moreover the average Ar/O value is −2.18 dex in excellent agreement with the Ar/O values of −2.18 dex and −2.22 dex for M17 and the Orion Nebula, respectively (Peimbert et al. 1992;

© Universidad Nacional Autónoma de México • Provided by the NASA Astrophysics Data System

1995RMxAA..31..147P

Peimbert 1993). The similar Ar/O values between Type I PNe and solar neighborhood H II regions imply that there is no O depletion in the shells of these objects due to nuclear reactions in the parent stars. Nevertheless in Figure 7 —where we present the O/H vs. $T(C^{++})$ diagram— there is a trend in the sense that the higher the $T(C^{++})$ value the lower the O/H value. This trend could be due to a real spread in the O/H values since the lower O/H the lower the cooling efficiency and the higher the $T(C^{++})$ value; alternatively it is possible that $T(C^{++})$ is still too high to determine the O^{++}/H^+ value and that a lower temperature should be used. This problem can be solved by determining O^{++}/H^+ based on highly accurate O II recombination line intensities.

The use of $T(C^{++})$ instead of $T(O^{++})$ increases the O^{++}/H^+ ratio of Type I PNe by factors between 2 and 3 because $T(C^{++}) \ll T(O^{++})$ (see Paper II), this increase in O^{++}/H^+ eliminates the difference between their O/H values and those derived from recently formed stars (e.g., Gies & Lambert 1992; Cunha & Lambert 1992; Cunha 1993).

5. CONCLUSIONS

By neglecting collisional and optical depth effects from the 2^3S level and considering a constant T_e we find discordant He^+/H^+ values from different He I lines.

By considering collisional and optical depth effects as well as the presence of spatial temperature fluctuations, the He^+/H^+ determinations based on different He I lines come into agreement. To reach this agreement there is no need to invoke an unknown mechanism to depopulate the 2^3S level.

The He I lines provide us with two new methods to determine T_e. These methods require highly accurate line intensity ratios.

Pairs of lines that depend weakly on collisional effects and that are almost independent of $\tau(3889)$ like $\lambda\lambda$5876 and 6678 or $\lambda\lambda$4471 and 5876 can be used to determine T_e in objects where collisional effects are extremely important, those with very high N_e and T_e values. The T_e results are practically independent of $\tau(3889)$.

Lines that depend strongly on collisional effects like $\lambda\lambda$3889, 7065 and 10830 can be used to determine T_e in objects where collisional effects are moderate, those with lower N_e or lower T_e values than the previous group. In this case it is also necessary to determine $\tau(3889)$, therefore we need to combine three He I lines. The best ones seem to be $\lambda\lambda$4471, 3889 and 7065 due to telluric absorption and dust destruction inside PNe of λ10830 photons.

The T_e (5876, 6678) and T_e (4471, 5876) values determined for Hu 1–2 , as well as the T_e (3889, 7065) values derived for the six non Type-I PNe presented in § 2.2, are considerably smaller than the $T_e(O^{++})$ values and similar to the $T_e(C^{++})$ values supporting the idea that $T_e(C^{++})$ is more representative than $T_e(O^{++})$ and probably that large temperature fluctuations are present inside PNe.

The Ne^{++}/O^{++} values derived for PNe of Type I probably are upper limits to the Ne/O value due to the presence of the charge exchange reaction $O^{++} + O^0 \rightarrow O^+ + H^+$ that allows some O^+ to coexist with Ne^{++}.

By determining the abundances of Type I PNe considering their high t^2 values, their O/H become similar to those of stars recently formed. Moreover their O^+/O^{++} ratios would become smaller, in better agreement with photoionization models.

The C/O values are larger than 1 for many objects; if lower T_e values are used then C^{++}/O^{++} would become smaller and also C/O. The smaller T_e values would imply even larger t^2 values.

Table 8 provides us with just a first approximation to the heavy element abundances of PNe of Type I. To derive better abundances for each of these objects we need a better knowledge of the temperature structure and detailed ionization structure models. Significant advances will be made if the abundances of some of these elements are derived from IR lines or from visual and UV recombination lines that are almost independent of the temperature structure.

It is a pleasure to acknowledge the referee for some excellent suggestions.

REFERENCES

Brocklehurst, M. 1972, MNRAS, 157, 211
Butler, S.E., Bender, C.F., & Dalgarno, A. 1979, ApJ, 230, L59
Clegg, R.E.S. 1993, in Planetary Nebulae, ed. R. Weinberger & A. Acker (Dordrecht: Kluwer), 549
Clegg, R.E.S., & Harrington, J.P. 1989, MNRAS, 239, 869
Cox, D.P., & Daltabuit, E. 1971, ApJ, 167, 257
Cunha, K. 1993, RevMexAA, 27, 111
Cunha, K., & Lambert, D.L. 1992, ApJ, 399, 586
Gies, D.R., & Lambert, D.L. 1992, ApJ, 396, 238
Harrington, J.P., Seaton, M.J., Adams, S., & Lutz, J.H. 1982, MNRAS, 199, 517
Hawley, S.A. 1978, PASP, 90, 370
Hawley, S.A., & Miller, J.S. 1977, ApJ, 212, 94
_____. 1978, PASP, 90, 39
Hummer, D.G., & Storey, P.J. 1987, MNRAS, 224, 609
Kaler, J.B., Shaw, R.A., & Kwitter, K.B. 1990, ApJ, 359, 392
Kingdon, J., & Ferland, G.J. 1991, PASP, 103, 752
_____. 1993, ApJ, 403, 211
_____. 1995, ApJ, 442, 714
Kingsburgh, R.L., & Barlow, M.J. 1994, MNRAS, 271, 257
Liu, X.-W., & Danziger, J. 1993, MNRAS, 263, 256
Mendoza, C. 1983, in IAU Symp. 103, Planetary Nebulae, ed. D.R. Flower (Dordrecht: Reidel), p. 143

© Universidad Nacional Autónoma de México • Provided by the NASA Astrophysics Data System

1995RMxAA..31..147P

Peimbert, M. 1971, Bol. Obs. Tonantzintla y Tacubaya, 6, 29
_____. 1993, RevMexAA, 27, 9
_____. 1995, in The Analysis of Emission Lines, ed. R.E. Williams & M. Livio (Cambridge: Cambridge Univ. Press), in press
Peimbert, M., & Costero, R. 1969, Bol. Obs. Tonantzintla y Tacubaya, 5, 3
Peimbert, M., & Torres-Peimbert, S. 1987a, RevMexAA, 14, 550 (Paper I)
_____. 1987b, RevMexAA, 15, 117
Peimbert, M., Torres-Peimbert, S., & Luridiana, V. 1995, RevMexAA, 31, 131 (Paper II)
Peimbert, M., Torres-Peimbert, S., & Ruiz, M.T. 1992, RevMexAA, 24, 155
Peña, M., Peimbert, M., Torres-Peimbert, S., Ruiz, M.T. & Maza, J. 1995, ApJ, 441, 343
Pequignot, D. 1980, A&A, 81, 356
Pequignot, D., Aldrovandi, S.M.V., & Stasińska, G. 1978, A&A, 63, 313
Robbins, R.R. 1968a, ApJ, 151, 497
_____. 1968b, ApJ, 151, 511
Robbins, R.R., & Bernat, A.P. 1973, Mémoires Societé Royale des Sciences de Liége, 6^e série, tome V, 263
Sawey, P.M.J., & Berrington, K.A. 1993, Atomic Data and Nuclear Data Tables, 55, 81
Shields, G.A., Aller, L.H., Keyes, C.D., & Czyzak, S.J. 1981, ApJ, 248, 569
Smits, D.P. 1991, MNRAS, 248, 193
_____. 1995, MNRAS, in press
Torres-Peimbert, S., Peimbert, M., & Daltabuit, E. 1980, ApJ, 238, 133

Valentina Luridiana, Manuel Peimbert, and Silvia Torres-Peimbert: Instituto de Astronomía, UNAM, Apartado Postal 70-264, 04510 México, D.F., México. (peimbert@astroscu.unam.mx).

© Universidad Nacional Autónoma de México • Provided by the NASA Astrophysics Data System